ESTIMATION OF DAMAGE LEVEL AT URBAN SCALE FROM SIMPLE PROXIES ACCOUNTING FOR SOIL AND BUILDING DYNAMIC PROPERTIES

C Salameh, P.-Y. Bard, B Guillier, C Cornou

16th World Conference on Earthquake Engineering, 16WCEE 2017
Santiago Chile, January 9th to 13th 2017
Paper N° 2049
Registration Code: S-W1463144195

ESTIMATION OF DAMAGE LEVEL AT URBAN SCALE FROM SIMPLE PROXIES ACCOUNTING FOR SOIL AND BUILDING DYNAMIC PROPERTIES

C. Salameh[(1)], P.-Y. Bard[(2)], B. Guillier[(3)], C. Cornou[(4)]

[(1)] *PhD, ISTerre- IRD, christelle.salameh@live.com*
[(2)] *PhD, ISTerre- IFSTTAR, pierre-yves.bard@ujf-grenoble.fr*
[(3)] *PhD, ISTerre- IRD, bertrand.guillier@ird.fr*
[(1)] *PhD, ISTerre- IRD, cecile.cornou@ujf-grenoble.fr*

Abstract

It has been observed repeatedly in the post-earthquake investigations that buildings having frequency similar to soil frequency (coming from H/V for example) exhibit significantly greater damage due to the double resonator concept (Caracas 1967, Mexico 1985, L'Aquila 2009). However this observation is generally not taken directly into account neither in present-day seismic regulations (small scale), nor in large-scale seismic risk analysis. We considered a theoretical analysis to study the effect of frequency coincidence between soil and building. As a first step, 887 natural soil profiles with linear behavior are associated to a set of single degree of freedom elastoplastic oscillators. The results obtained are used to quantify the damage increment related to the soil-building frequency coincidence and depending on different parameters such as the loading level characterized by the peak ground acceleration (PGA), the soil profile (impedance contrast, soil frequency) and the building (ductility, fundamental frequency). This statistical work is based on Artificial Neural Network (ANN) approach that does not require any prior knowledge, confirming that the main parameter controlling the damage increase is the ratio structure frequency to soil frequency (fstruct/fsoil), with a synaptic weight exceeding 58% (when PGA represents 27.05%, the impedance contrast 10.44% and ductility 4.24%). The leading parameter, i.e. the fstruct/fsoil ratio, controls also the damage increment when considering various ductility classes with a synaptic weight percentage of 45%; the parameter that follows is the PGA.

Keywords: spectral coincidence, frequency, damage, vulnerability, Neural Network, building.

1. Introduction

Most of the destructive effects of an earthquake come from vibrations associated to waves that are generated by a sudden slip along a fault. These vibrations are characterized by their frequencies and associated amplitudes, whereas waves are characterized by their type (body waves – compression or shear - and surface waves) and their velocity. The latter is relatively stable in the deepest layers, but highly variable when approaching the surface because it is directly related to the soil profile and bedrock. Therefore, the propagation of these waves is strongly affected by surface heterogeneities, and this spatial variability linked to geology is usually called "site effects". The amplitude and frequency characteristics have obviously an impact on the structural behavior. As a first approximation, a building can be considered as an "inverted pendulum", or as a cantilever embedded in soil: its vibratory behavior is similar to that of an oscillator with one or more degrees of freedom, and one or more vibration modes, and is characterized by its frequencies, mode shapes and damping; damages in a building are mostly related to internal deformations it undergoes, which in turn are linked to the total displacement imposed by the earthquake and the fundamental frequency of the building. If one of the soil frequencies coincides with the frequency of the building, and the incident energy is sufficient, the corresponding mode will be particularly activated, and the resulting deformation will be greater. Thus the coupling between resonators is a key parameter in the spatial distribution of damage during an earthquake, connected to the frequency distribution of soil and buildings, and the level of associated resonances (as a function of the rigidity contrast and the damping in soils and structures). This theoretical concept of a double resonator is repeatedly observed in post-seismic investigations (Caracas 1967, Mexico 1985, Pujili 1996): buildings with fundamental frequencies coinciding with the resonance frequencies of the soil are subjected to greater damage.

However, this observation is generally not taken into account neither in the current seismic regulations (small scale), nor in the analysis of seismic risk at urban scale. There is often a lack of consistency between the seismic risk studies that consider the actual frequencies of the ground, and the large-scale seismic risk maps that only account for the building frequency. Most often, the estimation of seismic hazards include the modeling of seismic actions based on local geological conditions, through a "site proxy ": the average velocity of S waves over a depth of 30 m, V_{s30}, is the most commonly used. Many recent studies emphasize the relevance of the fundamental frequency of soil as another potential "proxy", especially as its measurement is easily obtained by ambient vibration method (H/V method widely spread over the last two decades (Nakamura 1989 [1])). However, most of the seismic risk and vulnerability studies do not consider the dynamic parameters that could be easily extracted (Dunand 2005 [2]); instead they use traditional information such as the type and age of buildings to establish empirical formulas correlating damage to the macroseismic intensity at large scale.

The objective of this paper is to focus on the effects of the coincidence between soil and buildings frequencies, in order to derive an estimate of the damage increment, which could be applied to real sites where a lack of information on soil or structure does not allow an appropriate modeling of their behavior. In this perspective, a theoretical approach is undergone to establish both a mechanical understanding and a quantitative relationship between the expected damage and the various physical parameters related to the input seismic signal, and to the response of the soil foundation and the structure, considering the coincidence of frequencies. To that end, the Artificial Neural Network approach is used to analyze a large number of combinations composed of incident signals, realistic soil profiles and single degree of freedom buildings a; this approach does not require any prior idea on functional forms and connects the output parameter (increment of damage) to various input parameters (PGA, typology class, impedance contrast and frequency ratio structure/soil).

2. Realistic Case: Oscillator with a single-degree-of-freedom on a multi-layered profile

The study of the coincidence of frequencies between soil and structure involves the combination of a structure associated, a multilayered soil profile and a seismic signal injected at the base:

i. the seismic excitation considered here consists of a series of 60 synthetic realistic accelerograms for different scenarios (magnitude between 3 and 7, distance between 5 and 100 km, PGA from 0.02 $m.s^{-2}$ to 8.6 $m.s^{-2}$), that are simulated using Sabetta and Pugliese (1996 [3]) approach which has the particularity to (i) reproduce the real ground motion, by taking into account the nonstationarity of its amplitude and

frequency and (ii) generate multiple time histories having the same magnitude and distance source to site with a different random seed.

ii. 887 multilayer realistic soil profiles are compiled from KIKNET (Japanese site), Boore (California sites) and NERIES (European sites) database. Each soil profile is defined by a number of layers, and their thickness, Vp, Vs and density. In the absence of any further information about the quality factors Qp and Qs, we assumed Qp = 2Qs = Vs/5 (Aki and Richards 1980 [4]; Bertil et al. 1989 [5]).

iii. 141 oscillators with one degree of freedom with an elastoplastic behavior and realistic properties (Fig. 1) from the European Risk-UE project (Lagomarsino and Giovinazzi 2006 [6]): it covers a wide range of fundamental periods, elastic yield displacement, ductility coefficients; structures are classified into 5 main categories: Masonry, non-designed reinforced concrete reinforced concrete with Low (DCL), Medium (DCM), and High Ductility class (DCH)

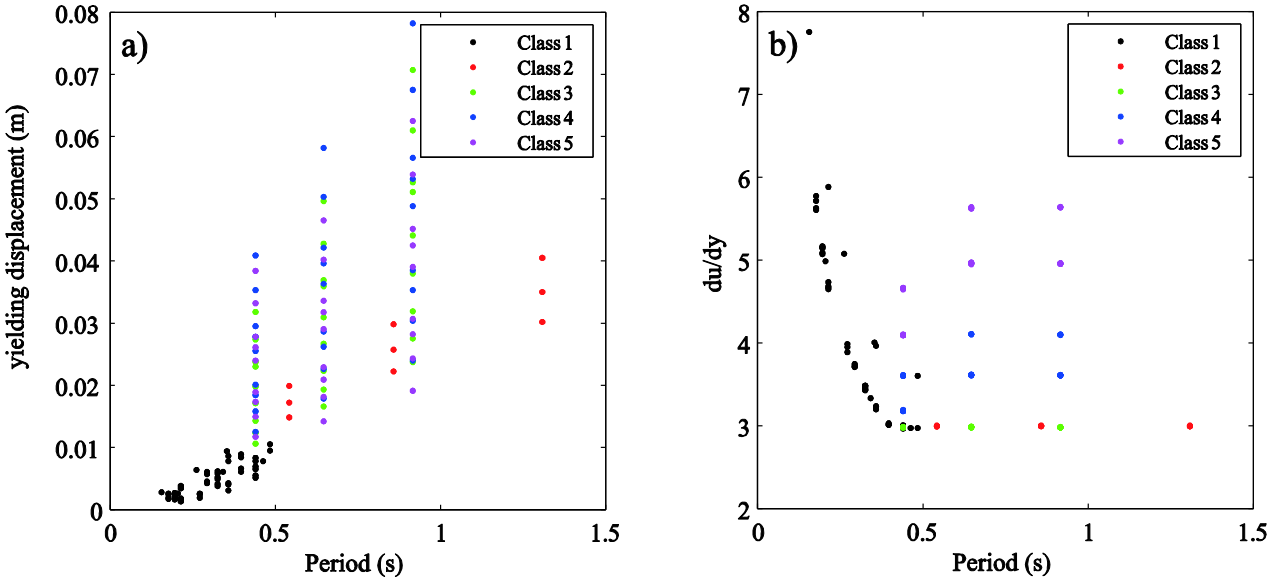

Fig. 1 – Distribution of the 141 structures taken from Lagomarsino and Giovinazzi (2006): a) yielding displacement dy (m), b) du/dy as a function of the period (s) with respect to the 5 typology classes.

A seismic signal is introduced and modified while propagating through the various layers of the soil medium due to the reflection and transmission mechanism at the interfaces (Kennet 1983 [7]). The signal modified at the soil surface is then injected at the base of the structure having an elastoplastic behavior without including the soil structure interaction. The equation of motion of a damped elastoplastic oscillator having a damping of 5% under a seismic excitation is solved by the step by step method of Newmark (Eq. (1)):

$$m\ddot{x} + c\dot{x} + kx = -m\ddot{x}_g \tag{1}$$

The maximum displacement at the top of the oscillator is thus obtained: if it is less than the elastic limit then the structure is not damaged and its behavior is in this case elastic; on the contrary if the maximum displacement exceeds the elastic limit, the structure enters the plastic range with irreversible damage. A total of 7504020 combinations (887 soil profiles x 60 seismic signals x 141 types of structure) are considered. For each model, maximum displacements are computed for two configurations: one where the structure is coupled to the soil foundation, and the other taking into account the same structure on the corresponding outcropping bedrock. A new index is designed to quantify the damage increment based on the European Risk-UE project (Lagomarsino and Giovinazzi 2006 [6]). The damage index D is a real number from 0 to 4 describing the state damage by comparing the maximum displacement of the structure with different displacement thresholds according to the following equations (Eq. (2)) and Fig. 2:

$$\begin{aligned}
&\text{no damage}: D0: dmax < 0.7dy, D = dmax/(0.7dy);\\
&\text{slight}: D1: 0.7dy < dmax < 1.5dy, D = 1 + (dmax - 0.7dy)/(1.5dy - 0.7dy);\\
&\text{moderate}: D2: 1.5dy < dmax < 0.5(dy + du), D = 2 + (dmax - 1.5dy)/[0.5(dy + du) - 1.5dy];\\
&\text{extensive}: D3: 0.5(dy + du) < dmax < du, D = 3 + [dmax - 0.5(dy + du)]/[du - 0.5(du + dy)];\\
&\text{complete}: D4: dmax > du, D = 4;
\end{aligned} \quad (2)$$

The next step is to statistically link the damage increment soil/rock ($\Delta DI=D_{soil}-D_{rock}$) to main input parameters: the frequency ratio structure/soil, the impedance contrast, the peak ground acceleration (PGA), the ductility. Given the huge number of results, the Artificial Neural Network approach is considered as a suitable technique to obtain correlations between these parameters without any prior assumption on functional forms that describe the dependency between parameters (Derras et al. 2012 [8]).

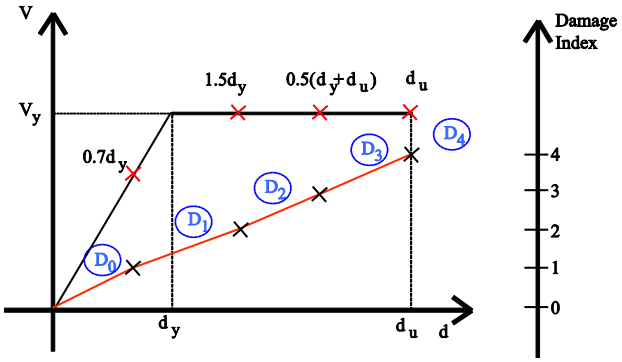

Fig. 2 – Damage index definition based on the damage state and displacements thresholds of Lagomarsino and Giovinazzi (2006 [6]).The black line is the capacity curve, the red line is the new damage index.

3. Artificial Neural Network (ANN) approach

3.1 Creating the network

The optimal neural network selected for this database (found after many trial) is a network composed of 4 input parameters: log (fstruct/fsoil), log (PGA), log (impedance contrast) and ductility (ratio of ultimate limit du over the yield dy); 1 output: the damage increment between soil and rock; with an intermediate layer of 15 'hidden' neurons. A preliminary training leads to the following synaptic weights percentages: 58% for the structure/soil ratio, 27.05% for PGA, 10.44% for the impedance contrast and 4.24% for the ductility. At first the leading parameter that controls the damage increment is the frequency ratio between structure and soil; since the ductility has the lowest impact, we neglect it as an input and considered only the first 3 inputs, however taking into account 5 neural networks with respect to the 5 typology classes already defined. The activation function is tanh sigmoid for the intermediate layer and linear for the output layer. The algorithm used is Broyden-Fletcher-Goldfarb-Shannoare BFGS (quasi -Newton method). The training is executed 10 times to ensure a good accuracy for the neural network due to the change in the initial conditions (weight and bias) at each training, and the problem of overfitting is avoided with the early stopping technique after randomly dividing each neural network into 3 data sets: 70% for training set, 15% for validation set and 15% for the test.

The input (I_n) and target (T_n) parameters are then normalized (Eq. (3)): This step is important to improve the efficiency of the training of the neural network and accelerate the computation process. The goal is to ensure that the extreme bounds of values for each net input and output are the same -1 and +1 (Meenakshi and Mohan 2012 [9]).

$$I_n = 2 \times \frac{I - I_{min}}{I_{max} - I_{min}} - 1$$

$$T_n = 2 \times \frac{T - T_{min}}{T_{max} - T_{min}} - 1 \quad (3)$$

I_{min} and I_{max}, T_{min} and T_{max} are respectively the minimum and maximum values for the input I_n and the target T_n.

The optimal number of hidden neurons is determined from the information criterion of Akaike (AIC) proposed by Akaike (1974 [10] and the root mean square error RMSE (Eq . (4), (6)). The more AIC and RMSE parameters are low, the better is the neural model (Fogel 1990 [11]; Murata et al. 1994 [12])

$$AIC = L \times \log MSE + 2 \times m \quad (4)$$

where

$$MSE = \frac{1}{L} \sum_{i=1}^{L} (d_l - y_l)^2 \quad (5)$$

$$RMSE = \sqrt{MSE} \quad (6)$$

with L: number of samples used for learning; m: number of synaptic weights in the network= (input+output) x hidden neurons; in other terms it is the number of degrees of freedom of the ANN, d_l is the normalized target value for the sample l and y_l is the normalized generated output by the ANN for the sample l. Fig. 3 shows that the optimal number of hidden neurons is equal to 10.

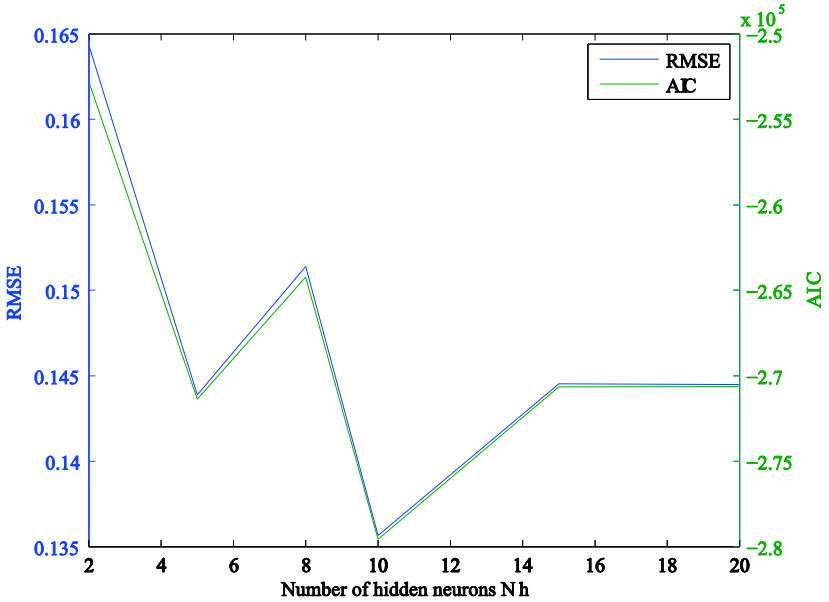

Fig. 3 – Choice of the number of neurons as a function of RMSE and AIC

The final architecture of the neural network is displayed in Fig. 4.

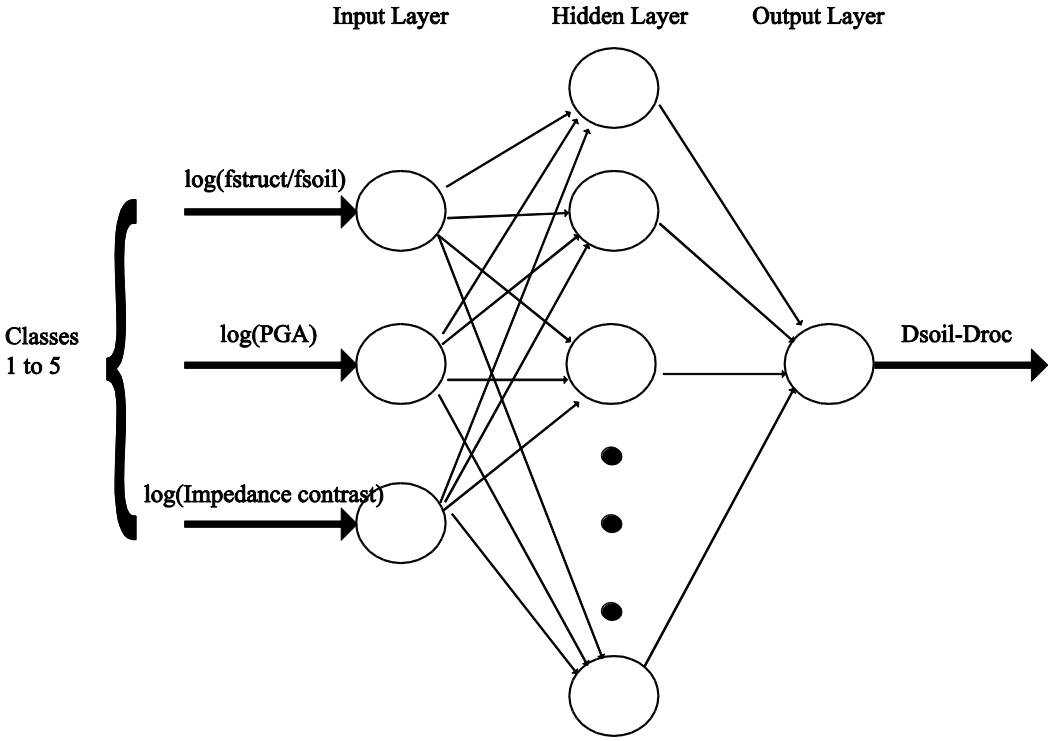

Fig. 4 – Architecture of the Neural Network for each of the 5 classes: inputs are the structure soil frequencies ratio, the impedance contrast and the PGA; the output is the damage increment between soil and rock.

3.2 Validating the network

The performance of the neural network is assessed based on statistical indicators (Longhi et al. 2005 [13]): the coefficient of determination (R^2) and the mean square error (MSE). Early stopping method is used to avoid overfitting. Table 1 summarizes the statistical parameters measuring the performance of the network (MSE and R^2) with respect to the 5 typology classes.

Table 1 – Statistical parameters measuring the performance of the network (MSE and R^2) with respect to the 5 typology classes.

	Standard deviation of normalized target	**All the data**		**Training (70%)**		**Validation (15%)**		**Test (15%)**	
		MSE	**RMSE**	**MSE**	**R^2**	**MSE**	**R^2**	**MSE**	**R^2**
Class1	0.1817	0.0157922	0.12566701	0.01581063	0.81158	0.01574783	0.81091	0.01575056	0.80836
Class2	0.17	0.01030307	0.10150402	0.01025234	0.80092	0.0106814	0.8012	0.01016147	0.80084
Class3	0.1724	0.01264732	0.11246029	0.01247183	0.80798	0.01260141	0.80808	0.01351214	0.80915
Class4	0.1525	0.00883103	0.09397356	0.00881253	0.80764	0.00893056	0.80543	0.00881781	0.80631
Class5	0.1473	0.00915062	0.09565889	0.00910931	0.81657	0.00926024	0.81543	0.00923381	0.80996

R^2 is about ~0.8 for the training (70%), validation (15%) and test (15%) sets, therefore this is an indication of a good fit and the model is thus validated.

3.3 Using the network

After building and validating the network, correlations between the inputs and outputs are determined based on matrices of weights and biases and on the predefined activation functions (tanh sigmoid and linear) according to the equation (Eq. (7)):

$$T_n = \phi_2[b2 + [w2] \times \phi_1[b1 + w1 \times I_n]] \pm \sigma \quad (7)$$

Where ϕ_1 and ϕ_2 are respectively the activation functions in the hidden (tangent sigmoid function) and the output layers (linear function); w1, b1, w2, b2 are respectively the matrices of weights and bias in the hidden and output layers.

Then in the post-processing phase inputs I and outputs O are denormalized using the same preprocessing parameters and based on Eq. (8):

$$I = \frac{1}{2} \times (I_n + 1) \times (I_{max} - I_{min}) + I_{min}$$

$$O = \frac{1}{2} \times (O_n + 1) \times (T_{max} - T_{min}) + T_{min} \quad (8)$$

Each input parameter that is introduced is initialized with an arbitrary weight: during the training process weights are updated in order to minimize the error between the computed output and the targets. Once the convergence occurs, the percentage of the synaptic weight for each input is computed based on Eq. (9):

$$P_i = \frac{\sum_{j=1}^{N_h} \left| w_{ij}^h \right|}{\sum_{i=1}^{N} \sum_{j=1}^{N_h} \left| w_{ij}^h \right|} (\%) \quad (9)$$

N: number of inputs, N_h: number of hidden neurons and w_{ij}^h synaptic weight between the i^{th} node of the input layer and the j^{th} node of the hidden layer.

Fig. 5 highlights the percentages of synaptic weights for each of the 3 input parameters considering the 5 typology classes: the most predominant parameter is the frequency ratio between soil and structure (~45%) whatever the typology class, which confirms the relevance of this parameter in the prediction of the damage increment. However it can be noted that the second significant parameter is the PGA (~30%), namely, the excitation level, and the last parameter (the lowest synaptic weight) is the impedance contrast (~20%).

Using the final matrices of weights and biases and replacing in the activation functions (Eq. [7]), we can compute the output (i.e. the damage increment between soil and rock) generated from the Neural Network as a function of the input variables considered. In this paper we considered only the class 3 (i.e. low ductility class DCL). The resulting graphs (Fig. 6) present the variation of the damage increment with respect to the structure/soil frequency ratio and the impedance contrast (C) (Fig. 6a, b), and the loading level (PGA) (Fig. 6c, d). Many observations can be noted when interpreting these graphs:

i. The effect of the spectral coincidence is clear with a peak of damages observed for fstruct/fsol= 1. The peak is less pronounced at intermediate PGA; however we can notice that for low ductility it is shifted towards high ratio of fstruct/fsoil at PGA >2 m/s^2: this can be explained by the fact that at high PGA the structure enters the plasticity domain: its frequency is thus decreased and its

damping increased and the frequency coincidence can thus occur for originally stiffer degrading buildings.

ii. When the impedance contrast increases the damage increment increases because of the increase of the soil amplification.

iii. When PGA increases the damage increment increases as expected due to the level of excitation.

Thus, the Neural Network can estimate the damage increment from the information about 4 parameters: PGA on the rock (a proxy for an earthquake scenario), ductility (the typology of the building), the velocity contrast (a proxy for the amplification of the soil) and the frequency ratio. The latter is relatively easy to measure or predict from the ambient vibration measurements. A final major conclusion is made by comparing the standard deviation of the desired normalized targets and the standard deviation RMSE of the generated output from the ANN in Table 1: we can notice for all typology classes that the initial standard deviation was reduced to almost 30~50% of its value; this confirms the performance of the Neural Network to better fit the data available highlighted by a very good coefficient of determination R^2.

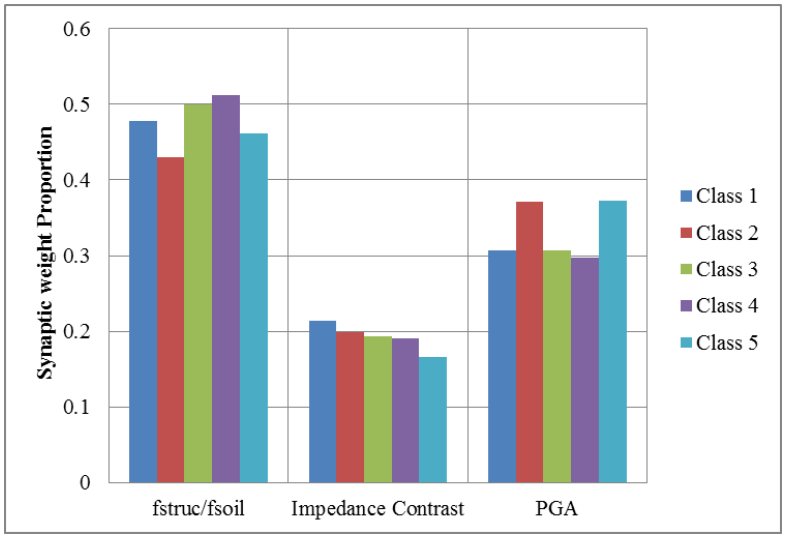

Fig. 5 – Synaptic weights percentage distribution according to the input parameters and the typology classes.

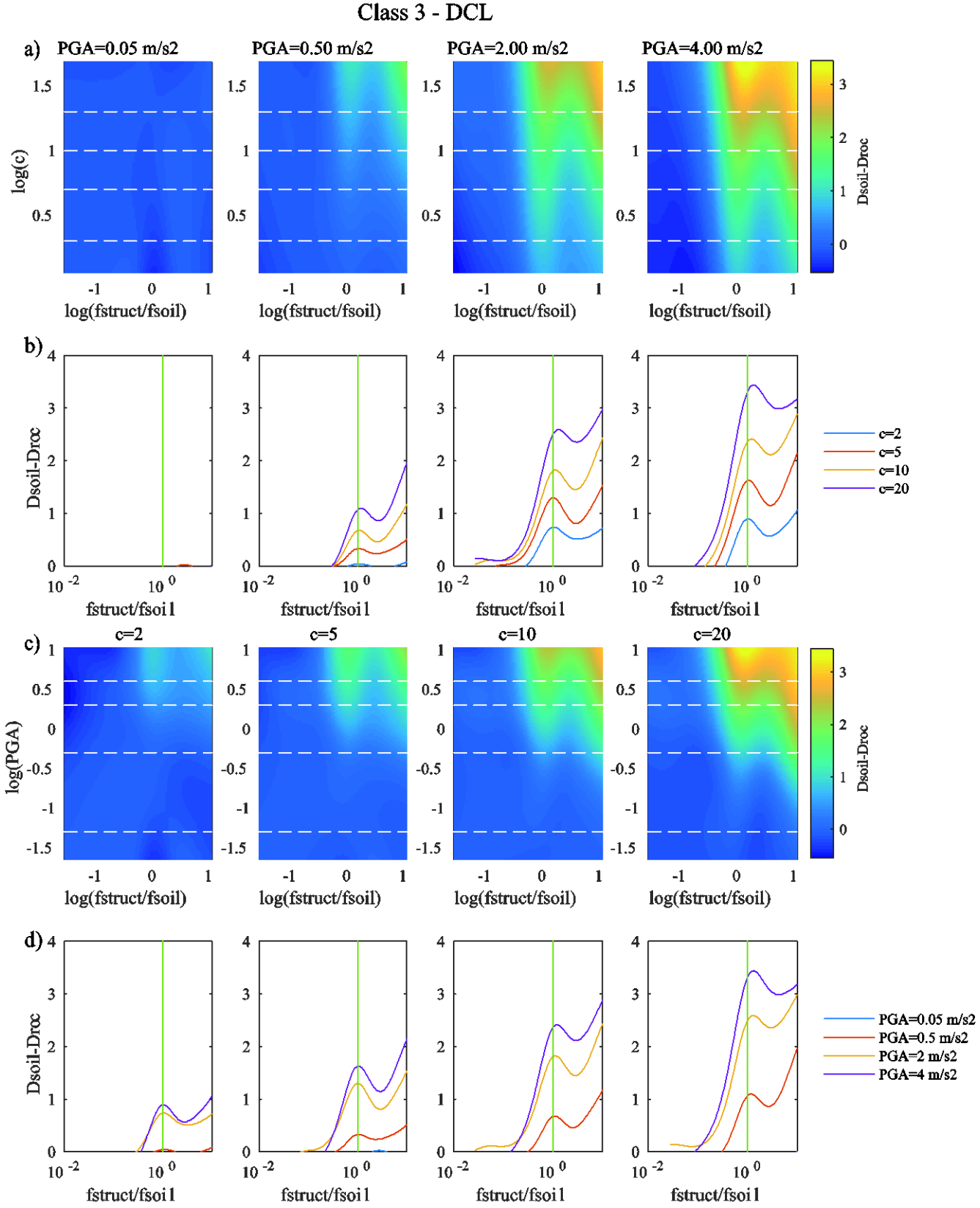

Fig. 6 – Class 3:Variation of the damage increment between soil and rock as a function of the structure to soil frequency ratio and: a) the impedance contrast , and b) for 4 values of c, for different ranges of PGA (m/s2); c) the PGA (m/s^2), and d) for 4 values of PGA , for different ranges of contrast.

4. Conclusion

The effect of the spectral coincidence between soil and structure is investigated using the response of a simple oscillator with a perfect elastoplastic behavior (defined by: the elastic limit, the fundamental frequency, the ductility) associated to a multilayer soil profile (characterized by two key parameters: the impedance contrast, and fundamental frequency) and a series of synthetic accelerograms mimicking an earthquake with a variable range of distances and magnitudes (related to the peak ground acceleration PGA and spectral content). Structural damage is defined as the ductility demand (ratio of the maximum displacement with respect to the elastic limit), and the damage increase due to the soil amplification is quantified by comparing the ductility when the same elastoplastic oscillator is on the soil or on the outcropping bedrock. Hundreds of realistic soil profiles are considered to explore the effects of spectral coincidence on damage considering a wide range of typologies of conventional construction from Risk-UE project. A new damage index was introduced to quantify the increment damage due to amplification of the soil. The large number of results (over 7.5 million) led us to use a Neural Network approach to explore the dependence of damage on mechanical properties of the soil and structure. Despite the absence of any prior functional form, it was confirmed that the key parameter that controls the damage increment is the ratio fstruct/fsoil with a synaptic weight close to 45%. The effect of this spectral coincidence between the soil and the structure is very clear at moderate PGA with a pronounced peak at fstruct/fsoil = 1. This interesting tool (Neural Network), which is not only used in seismology but in many other fields, proved to be an ad hoc tool to analyze our large dataset of soil/structures/signals and to highlight the most impacting parameter (the coincidence of frequencies) in the estimation of the buildings "damage". The reduction of the standard deviation in the target set by almost 30~50% when computing the generated output, highlights the efficiency of the Neural Network and its high capacity of performing and fitting the model. This efficiency is also demonstrated by investigating the mean squared errors MSE and the coefficient of determination R^2 which show very good values and the relevancy of the selected parameters as well. An important next step would be to find a proxy for the amplification of the soil that would be measured more easily, namely the H/V amplitude obtained from ambient noise measurements instead of the impedance contrast that needs geotechnical testing which is less economic and more difficult to acquire. Another direction for further investigations would be to look for other sets of site and building parameters that could lead to a larger variance reduction. However, in view of applications at an urban scale, one must always search the optimal compromise between physical relevance and practical considerations (i.e., the easy availability of the selected parameters).

5. Acknowledgements

This work was supported by the research program (ANR Libris 2010-2014) in collaboration with ISTerre laboratory (Grenoble, France), Notre Dame University- Louaize NDU, and is partially funded by IRD (Institut de recherche pour le développement). The authors also thank Boumédiène Derras for his help and advice in the Artificial Neural Network approach.

6. References

[1] Nakamura, Y. (1989). A method for dynamic characteristics estimation of subsurface using microtremor on the ground surface. Quaterly Report Railway Tech. Res. Inst., 30(1), 1-14.

[2] Dunand, F. (2005). Pertinence du bruit de fond sismique pour la caractérisation dynamique et l'aide au diagnostic sismique des structures de génie civil. PhD thesis, Université Joseph-Fourier- Grenoble I.

[3] Sabetta, F., & Pugliese, A. (1996). Estimation of response spectra and simulation of nonstationary earthquake ground motions. Bulletin of the Seismological Society of America, 86 (2), 337-352.

[4] Aki, K., & Richards, P. G. (1980). Quantitative Seisimology: Theory and Methods (Vol. 1). Freeman.

[5] Bertil, D., Bethoux, N., Campillo, M., & Massinon, B. (1989). Modeling crystal phases in southeast France for focal depth determination. Earth and Planetary Science Letters, 95(3), 341-358.

[6] Lagomarsino , S., & Giovinazzi, S. (2006). Macroseismic and mechanical models for the vulnerability and damage assessment of current buildings. Bulletin of Earthquake Engineering, 4(4), 415– 443.

[7] Kennet, B. (1983). Seismic wave propagation in stratified media. . Cambridge University Press.

[8] Derras, B., Bard, P.-Y., & Cotton, F. (2012). Adapting the neural network approach to PGA prediction: an example based on the KiK-net data. Bulletin of the Seismological Society of America, 102(4), 1446-1461.

[9] Meenakshi, A., & Mohan, V. (2012). Knowledge management in edaphology using self organizing map (SOM). International Journal of Database Management Systems, 4(5), 91.

[10] Akaike, H. (1974). A new look at the statistical model identification. Automatic Control, IEEE Transactions on, 19(6), 716-723.

[11] Fogel, D. B. (1990). Fogel, D. B. (1990). An information criterion for optimal neural network selection. IEEE transactions on neural networks/a publication of the IEEE Neural Networks Council, 2(5), 490-497.

[12] Murata, N., Yoshizawa, S., & Amari, S. I. (1994). Network information criterion-determining the number of hidden units for an artificial neural network model. Neural Networks, IEEE Transactions, 5(6), 865-872.

[13] Longhi, S., Nijkamp, P., Reggianni, A., & Maierhofer, E. (2005). Neural network modeling as a tool for forecasting regional employment patterns. International Regional Science Review, 28(3), 330-346.